

34

# N79-17509

USING MODEL ORDER TESTS TO DETERMINE SENSORY INPUTS IN A MOTION STUDY\*

D. W. Keppinger  
A. M. Junker

Aerospace Medical Research Laboratory  
Wright-Patterson Air Force Base, Ohio 45433

### ABSTRACT

In the study of motion effects on tracking performance, a problem of interest is the determination of what sensory inputs a human uses in controlling his tracking task. In the approach presented here a simple canonical model (PID or a proportional, integral, derivative structure) is used to model the human's input-output time series. Using a test discussed by Astrom [1], a study of significant changes in reduction of the output error loss functional is conducted as different parameters of the model are considered. Since this canonical model includes parameters which are related to inputs to the human (such as the error signal, its derivatives and integration), the study of model order is equivalent to the study of which sensory inputs are being used by the tracker. The parameters are obtained which have the greatest effect on reducing the loss function significantly. In this manner the identification procedure converts the problem of testing for model order into the problem of determining sensory inputs.

The research reported in this paper was sponsored by the Aerospace Medical Research Laboratory, Aerospace Medical Division, Air Force Systems Command, Wright-Patterson Air Force Base, Ohio 45433. This paper has been identified by the Aerospace Medical Research Laboratory as AMRL-TR-77- . Further reproduction is authorized to satisfy needs of the U. S. Government.

### 1. Introduction

The study of the effects of motion on human tracking performance is an area which has achieved increased emphasis and importance in the Air Force. One example of this need is in a quantitative assessment of how a pilot's control behavior is modified by the presence of motion cues which has immediate application in the area of motion base simulator design.

At the Aerospace Medical Research Laboratory (AMRL), Wright-Patterson Air Force Base, Ohio, an extensive motion program is currently being conducted to study many of the different aspects of motion effects on the human involved in a tracking task. The roll axis tracking task at AMRL was investigated for a variety of plant dynamics and has been documented in [2] and [3]. An extension of the Roll Axis Tracking Study was the peripheral display experiment which has been discussed in [4], [5], and [6], with an application of modeling in [7].

Recently at AMRL the study of motion effects has been extended to investigate the effects of washout in an improved version of the Roll Axis Tracking Simulator. A study of washout effects will answer the question as to the credibility of a ground base simulator as compared to the actual flight mission. A second simulator called the Multi Axis Tracking Simulator (MATS) has been recently added to AMRL and this simulator has the capability of providing motion in the roll, pitch, and yaw axes. By using the MATS and applying the Bolt Beranek and Newman (BBN) optimal control model to determine those experimental design conditions which would give rise to performance changes, a study was run [8,9] in which the model predicted experimental results prior to executing the experiment.

The model predictions were within one standard deviation of the means of the experimental results for approximately 80% of the experimental

variables considered. These results were averaged across six subjects involved in four tracking tasks. The data base was taken from the MATS experiment for this paper to investigate a modeling approach based on a simple canonical model to model the PID or Proportional Integral Derivative modeling approach.

#### II. Motivation for Using a Simple Canonical Model

In the study of manual control problems in which data has already been collected there exists several advantages in studying data when model parameters can be expressed in a PID formulation. The primary motivation for such a representation of a human is in the quantification of the ability of the human to differentiate (lead generation).

Figure (a) illustrates the man-in-the-loop problem considered here. For the purposes of analysis, the time series variables that are available for modeling are illustrated in figure (1b). The displayed error signal  $e(t)$  which is the input to the man is also the input time series to the computer model. The output time series of the man is denoted as  $ST(t)$ . The computer model has an output  $\hat{ST}(t)$  which is the best (in the sense of least squares) estimate of  $ST(t)$  based on the structure of the model assumed and the available data  $e(t)$  and  $\hat{ST}(t)$ . This type of modeling is termed output error because the difference between two time series outputs are considered. The modeling error is denoted as  $e_M(t)$  and it satisfies

$$e_M(t) = ST(t) - \hat{ST}(t) \quad (1)$$

The objective of this identification procedure is to choose a transfer function  $H(s)$  to minimize the output error loss functional  $J$  denoted as:

$$J = \frac{1}{N} \sum_{i=1}^N [e_M(t_i)]^2 \quad (2)$$

where  $N$  is the number of samples of data.

The choice of the canonical model  $H(s)$  is the primary motivation for the approach presented in this paper. If  $H(s)$  can be chosen in a manner such that

the human can be characterized by parameters which quantify the amount of differentiation or lead generation in a tracking task, then this model has application in the study of manual control problems. In addition, it will be shown in the sequel, that for each possible displayed variable (such as  $e(t)$ ,  $\dot{e}(t)$ , and  $\ddot{e}(t)$ ), a noise source associated with these displayed variables can be determined. First the canonical model will be specified as follows:

$$H(s) = \frac{a_0 + a_1 s + a_2 s^2 + a_3}{(1 + s/a)^3} \quad (3)$$

where  $s$  is the Laplace transform variable. Equation (3) is an ideal representation of the man-in-the-loop for several reasons. The coefficients  $a_0$ ,  $a_1$ , and  $a_2$  represent differentiation (or lead generation) in the tracking task. Therefore, instead of giving heuristic arguments as to whether the describing function of the man has more lead in one experimental condition as compared to another, the coefficients  $a_0$ ,  $a_1$ , and  $a_2$  will quantitatively indicate this fact. Also, the coefficient  $a_3$  allows the consideration of precognitive effects in a quantitative manner. The coefficient  $a$  in equation (3) is used to generate a third order pole for some value of a greater than 10 radians. This allows the transfer function  $H(s)$  to have a denominator with a higher order polynomial of  $s$  than the numerator and hence can be realized using state variables. The form of equation (3) allows the transfer function  $H(s)$  to have any amount of lead (including up to double differentiation) for frequencies from 0 to a radians. The amount of lead generation will depend on the numerical values of the coefficients  $a_0$ ,  $a_1$ , and  $a_2$ .

Another interpretation of the transfer function  $H(s)$  in equation (3) can be seen in Figure (2). In Figure (2) the man is replaced by a parallel processing channel which describes the input signal  $e(t)$  and the output signal  $ST(t)$ . The coefficients  $a_0$ ,  $a_1$ ,  $a_2$  and  $a_3$  indicate with what importance this

### III. Implementation of This Identification Procedure

In reference [7], an identification approach was applied to roll axis tracking data for a specified choice of state variables. In [7] it was difficult to validate the model because of the complex manner of the implementation procedure. This paper will illustrate a much simpler manner of implementing a PID type model and, in addition, provide several ways to validate such a model. Figure 3 illustrates the implementation procedure used in this paper which is equivalent to the diagram in Figure (2). The first step in the implementation procedure is to determine the prefiltered variables  $\hat{e}(t)$ ,  $\hat{\dot{e}}(t)$ , and  $\int_0^t e(\tau) d\tau$  by the following realizable transfer functions (capital letters indicate Laplace Transform Variables):

$$\hat{E}(s) = E(s) \quad (6a)$$

$$\frac{\hat{\dot{E}}(s)}{E(s)} = \frac{s}{(1 + s/a_0)^2} \quad (6b)$$

$$\frac{\hat{\int} E(s)}{E(s)} = \frac{s^2}{(1 + s/a_0)^2} \quad (6c)$$

$$\int_0^t \hat{e}(\tau) d\tau = 1/s \quad (6d)$$

Equations (6a-d) are easily implemented by using digital filter techniques. The identification stage of this implementation procedure requires the choosing of state variables so that  $a_0$ ,  $a_1$ ,  $a_2$ , and  $a_3$  can be obtained. In the identification procedure, the following relationship holds:

$$ST(t) = ST_1(t) + ST_2(t) + ST_3(t) + ST_4(t) + \xi_1 + \xi_2 + \xi_3 + \xi_4$$

To implement these equations choose state variables:

$$x_1 \stackrel{\Delta}{=} ST_1(t) \quad (7a)$$

$$x_2 \stackrel{\Delta}{=} ST_2(t) \quad (7b)$$

$$x_3 \stackrel{\Delta}{=} ST_3(t) \quad (7c)$$

$$x_4 \stackrel{\Delta}{=} ST_4(t) \quad (7d)$$

particular time signal is converted or processed into the stick signal  $ST(t)$ . If  $a_2 \gg a_0$  and  $a_2 \gg a_1$  then one would expect the signal  $ST(t)$  to be dominated by double differentiation of  $e(t)$ . On a log-log plot of  $\frac{ST(s)}{E(s)}$ , one would expect to see second order lead characteristics. Also, in Figure (2) the vector white noise sources  $\xi_1(t)$ ,  $\xi_2(t)$ ,  $\xi_3(t)$ , and  $\xi_4(t)$  have special significance. These noise sources can be determined by identifying the coefficients  $a_0$ ,  $a_1$ ,  $a_2$ , and  $a_3$  and injecting the modeling error into these noise sources. This approach is similar to the vector white noise Kemant Model proposed by Levison, Baron, and Kleinman [10] which has been validated experimentally. In the approach presented here the modeling error is generally a fixed percent of the magnitude (usually 5-10%) of the unknown coefficients ( $a_0$ ,  $a_1$ ,  $a_2$  or  $a_3$ ). Let  $\beta$  denote the percent of modeling error for a specific parameter (for example,  $a_0$  in Figure (2) which corresponds to an input  $e(t)$ ), then:

$$\xi_1(t) = \beta a_0 e(t) \quad (8)$$

For a time history an integral multiple of the periods of the sine waves, the following mean and variance of  $\xi_1(t)$  results:

$$\xi_1 \text{ mean} = 0 \quad (5a)$$

$$\text{Var} \{ \xi_1(t) \} = \beta^2 a_0^2 \text{Var} \{ e(t) \} \quad (5b)$$

Therefore, the variance of the noise sources  $\xi_1(t)$  scales in proportion to the input channel error variance. This type of scaling of the noise variances in proportion to the variance of that component of the displayed error signal is what is desired. This Weber's law scaling effect has been discussed by Jex et al. [11] for an equivalent scalar injected noise source at the observation point of the human operator in the loop. Therefore, this approach allows uncorrelated human response to scale in proportion to the perceived variable. The implementation of this identification procedure is now presented to describe in detail the manner of computing the unknown parameters.

Then

$$\frac{X_1(s)}{\dot{E}(s)} = \frac{a_0}{1 + s/a} \quad (8a)$$

$$\frac{X_2(s)}{\dot{E}(s)} = \frac{a_1}{1 + s/a} \quad (8b)$$

$$\frac{X_3(s)}{\dot{E}(s)} = \frac{a_2}{1 + s/a} \quad (8c)$$

$$\frac{X_4(s)}{\int_0^t \dot{E}(\tau) d\tau} = \frac{a_3}{1 + s/a} \quad (8d)$$

The implementation of equations (8a-d) proceeds as follows:

$$\begin{bmatrix} \dot{X}_1 \\ \dot{X}_2 \\ \dot{X}_3 \\ \dot{X}_4 \end{bmatrix} = \begin{bmatrix} X_1 \\ X_2 \\ X_3 \\ X_4 \end{bmatrix} + \begin{bmatrix} a_0 \\ a_1 \\ a_2 \\ a_3 \end{bmatrix} \begin{bmatrix} e(t) \\ \dot{e}(t) \\ \ddot{e}(t) \\ \int_0^t e(\tau) d\tau \end{bmatrix} \quad (9a)$$

$$ST(t) = [1, 1, 1, 1] \begin{bmatrix} X_1 \\ X_2 \\ X_3 \\ X_4 \end{bmatrix} + \sum_{i=1}^4 f_i f_i(t) \quad (9b)$$

Therefore, the variable  $s$  is just the prefiltering variable, the unknowns are  $a_0, a_1, a_2,$  and  $a_3$  which are determined from a least squares identification algorithm. The PID identification algorithm is determined by identifying  $a, a_0, a_1, a_2,$  and  $a_3$ .

In this implementation, the time series  $e(t)$  was delayed by 0.20 seconds,  $\dot{e}(t)$  was delayed by 0.12 seconds, and  $\ddot{e}(t)$  was delayed by 0.04 seconds. The

manner of achieving these delays was accomplished by shifting the real time series by an integral multiple of the sampling rate (.04 seconds). The assumption of different delays on the perceptual variables is perhaps a better assumption than a single, constant delay on all four channels.

In the case of tracking with a motion disturbance it is reasonable to assume that information from rates and accelerations may be processed more rapidly than position information. Since the desire of this paper is to produce a lumped representation of a human, these lags were chosen over four experimental conditions of the motion experiment. Once this model is sufficiently validated, future work can be done to investigate the lags of each individual channel and for the different experimental conditions considered here.

A description of the MATS experiment and data base used for this study is next presented.

#### IV. The Multi-Axis Tracking Simulator (MATS)

Figure (4) illustrates a physical diagram of the MATS. A brief description of this simulator will be presented here. A more complete description can be found in [8,9].

The MATS simulator was used only in the roll axis for this study with two independent inputs:  $\phi$  TARGET and  $\phi$  DISTURBANCE as indicated in Figure (4). Four modes of tracking were conducted:

- (1) STATIC DISTURBANCE  
 $\phi$  Target = 0 with  $\phi$  Disturbance  $\neq$  0 with no motion
- (2) MOTION DISTURBANCE  
 $\phi$  Target = 0 with  $\phi$  Disturbance  $\neq$  0 with roll motion
- (3) TARGET STATIC  
 $\phi$  Target  $\neq$  0 with  $\phi$  Disturbance = 0 with no motion
- (4) TARGET MOTION  
 $\phi$  Target  $\neq$  0 with  $\phi$  Disturbance = 0 with roll motion

Another measure of performance is the variances of the error, error rate, and error acceleration. For the disturbance input case these variables became the plant position, rate and acceleration with just a  $-180^\circ$  sign change in this signal. These variables were calculated and averaged across subjects. The results of these time series answers are displayed in Table II.

TABLE II

	TARGET MOTION	TARGET STATIC	DISTURBANCE MOTION	DISTURBANCE STATIC
$\sigma_e$	6.90	7.06	4.2	8.83
S.D.	0.78	0.74	1.5	1.80
$\sigma_{\dot{e}}$	11.8	11.9	6.81	11.9
S.D.	0.79	0.7	1.41	1.3
$\sigma_{\ddot{e}}$	40.02	59.522	24.0	33.6
S.D.	15.161	8.33	1.9	5.0

The numerical values in Table II are also measures of performance which are an important aspect of this experiment.

V. Parametric Results From the Identification Algorithm:

Using various values of  $\alpha = 5$  to  $\alpha = 50$  radians, the identification scheme was applied to the time series data  $e(t)$  and  $ST(t)$  over the four conditions of motion inputs. Table III illustrates the resulting parametric values for  $\alpha = 20$ .

In order to show that such a model has credibility it was validated two different ways. The purpose of a validation is to demonstrate that this lumped, simplified model can adequately represent the human in the tracking task. Model order tests were used to determine which parameters (or inputs) to the human had the greatest effect in reducing the output error loss functional of equation (2). In the following sections we present the validation results and parameter sensitivity tests.

The two input spectrums (Target and Disturbance) were designed based upon a priori guesses of inputs that gave rise to performance changes as indicated by the BVA optimal control pilot vehicle model. Figure (5) is a plot of the two input spectrums. The effective plant dynamics controlled by the subjects was specified by:

$$G(s) = \frac{10.0}{s(1 + s/5)(1 + s/20)} \quad (10)$$

The subjects involved in the experiment were six college students (male and female) 18-25 years of age. The subjects tracked each of the four experimental conditions for 165 seconds each day with the runs presented in a random sequence. The subjects were told to minimize the following score:

$$J = \text{Score} = \sigma_e^2 + \text{error} + 0.1 \sigma_{\dot{e}}^2 + \text{plant} \quad (11)$$

At the end of each run the subjects were told the score,  $\sigma_e^2$  error, and  $0.1 \sigma_{\dot{e}}^2$  plant. They were instructed to minimize the total score. When the scores reached asymptotic levels, subject training was assumed to be accomplished. The experiment was then run for an additional eight days and data was collected. The performance results are summarized in Table I for the eight days of collected data.

TABLE I

	TARGET MOTION	TARGET STATIC	DISTURBANCE MOTION	DISTURBANCE STATIC
$J$ (Score)	66.1	72.8	78.6	197.0
S.D.	7.5	8.9	15.5	29.0
$e^2_{RMS}$	46.25	56.4558	16.248	66.6688
S.D.	13.2547	11.45249	8.910	16.71518

One can see from Table I that in the disturbance mode of operation the effects of motion on performance were quite profound. In the target mode of operation the effects of motion were not that pronounced.

TABLE III -  $n = 20$

	TARGET MOTION	TARGET STATIC	DISTURBANCE MOTION	DISTURBANCE STATIC
$a_0$ Mean	.0526004	.090132	-.4435146	-.161338667
S.D.	.008456306	.00710845	.050885703	.02343810
$a_1$ Mean	.00397449	.00590767	-.1121918	-.01287437
S.D.	.0028907	.00352572	.015809079	.0058299
$a_2$ Mean	.0002010	-.000782808	-.00121983	.0136601
S.D.	.0003102	.000462707	.00130466	.001958
$a_3$ Mean	-.003723948	-.0002520066	.001752651	.0054614711
S.D.	.0006512954	.000767361145	.0030386457	.001072189

VI. Two Methods of Model Validation

The lumped model developed here was validated in the frequency domain and also in the time domain. The first method of model validation was a comparison of averaged values of spectra plots (Fast Fourier Transforms) to averaged values of the PID parameters. In this manner a spectra identification procedure is compared to a parametric identification algorithm. Using a Fast Fourier Transform program developed at ANRL, ensemble averages of the spectra of the time series  $e(t)$  and  $ST(t)$  were obtained for the four tracking tasks considered here. In addition, the parametric plots of Table III were obtained for the mean values of the parameters and two additional plots of the mean values of the parameters  $\pm 1$  standard deviation; these parameter values. Since the describing functions obtained from the FFT's were also plotted as mean values  $\pm 1$  standard deviation of each spectra estimate, the two ensemble plots can be overlaid and compared.

Figures (6), (7), (8), and (9) illustrate the plots of the two identification schemes overlaid. The results of Figures (6-9) indicate that the two schemes match best for the case of static disturbance and motion disturbance conditions. For the static target and motion target case, the two identification schemes match with less consistency.

In all four cases the uncertainty envelope obtained from one standard

deviation of the parametric plots about their mean when overlaid with the corresponding envelope obtained from the spectra plots, results in overlap of these envelopes. One interpretation of this result is that the uncertainty in the parametric estimation scheme is no worse than the uncertainty in the spectra estimates.

The second method of model validation is to consider how well the time series  $\hat{ST}(t)$  generated from the computer model matches the experimental time history data  $ST(t)$ . The ratio R given in equation (12) is a measure of this match. The ratio considered is

$$R = \left[ 1 - \frac{\sum_{i=1}^N [ST(t_i) - \hat{ST}(t_i)]^2}{\sum_{i=1}^N [ST(t_i)]^2} \right] \quad (100\%) \quad (12)$$

This variable is calculated and the results are displayed in Table IV.

TABLE IV

	TARGET MOTION	TARGET STATIC	DISTURBANCE MOTION	DISTURBANCE STATIC
R mean	89.98%	94.76%	95.36%	95.94%
R S.D.	1.6084	.86197	1.5274	1.1502

From the results of Table IV we can see that there is a high correlation between the model output time series and the output series from the empirical data.

It is now of interest to complete a sensitivity study on which parameters ( $a_0, a_1, a_2$ , or  $a_3$ ) will reduce the output error for functional of eq. 2. For the PID model developed here, the parameter which is most sensitive will indicate which of the possible inputs  $e(t), \dot{e}(t), \ddot{e}(t)$ , or  $\int_0^t e(\tau)d\tau$  is most important in describing the input-output characteristics of the human as a parallel processor of information. In this manner some insight can be obtained as to which input

sensory variable may be used by the human when he is represented in Figure (2).

VII. Using Model Order Tests to Validate the Model and to Determine

Sensory Inputs To The Human

In an effort to investigate which sensory inputs are used by the human in the tracking task, two tests on the correct model order were considered. The two tests considered were Astrom's F-Ratio test [1] and a parameter consistency test [12] used in the mathematical bio-sciences literature. Before any tests are conducted, it is necessary to calculate values of the output error loss functional for different combinations of input parameters. In order to obtain a table of output error loss functional values, the following sequence of steps was performed on one experiment from each of the four motion modes of operation:

- (1) Assume the human can be represented by one parameter.
- (2) Calculate the loss functional  $J_1$  of equation (2) for one parameter.
- (3) Now assume the human can be represented by two parameters.
- (4) Calculate  $J_2$  for the two parameter case.
- (5) Assume the human is represented by 3 parameters.
- (6) Calculate  $J_3$ .
- (7) Assume all four parameters characterize the human.
- (8) Calculate  $J_4$ .

Using Astrom's test [1], a measure of which parameter significantly reduces the loss functional was conducted. Table V lists the values of the loss functional obtained here.

Since Table V contains many entries due to the numerous combinations of parameters considered here, it is desirable to study which patterns of parameters are important to investigate. The index of parameter consistency developed in [12] provides a method of simplifying the results in Table V. The following

TABLE V - VALUES OF LOSS FUNCTION

	TARGET MOTION	TARGET STATIC	DISTURBANCE MOTION	DISTURBANCE STATIC
$J_1 =$				
One Parameter Loss Function	$a_0$			
	$a_1$	.6274	.7576	.6249
	$a_2$	1.075	1.516	1.514
	$a_3$	.7532	1.564	1.241
	$a_0, a_1$	1.064	1.567	1.430
	$a_0, a_2$	.3909	.7208	.6136
	$a_0, a_3$	.5226	.6792	.6043
	$a_1, a_2$	.6040	.7099	.6130
	$a_1, a_3$	.7501	1.468	1.192
	$a_2, a_3$	1.064	1.439	1.349
	$a_0, a_1, a_2$	1.536	1.536	1.121
	$a_0, a_1, a_3$	.2590	.5561	.5991
	$a_0, a_2, a_3$	.3205	.6922	.4123
	$a_1, a_2, a_3$	.7483	1.401	1.004
L.F.	$a_0, a_1, a_2, a_3$	.5094	.6091	.3838
$J_4$	$a_0, a_1, a_2, a_3$	.2697	.5030	.3784

index of parameter consistency was used [12]:

$$\text{index} = \frac{1}{M} \sum_{i=1}^M \frac{c_i}{u_i} \quad (13)$$

where  $M$  = the number of parameters considered,  $c_i$  is the standard deviation of the parameter, and  $u_i$  is the mean value of the absolute value of this parameter. According to the test in [12], this index of consistency is smallest when the correct system order is determined. Table VI lists the calculations of this index of consistency for the parameters displayed in Table III.

From Table VI it can be seen that when the parameter  $a_3$  is included with any other group of parameters, the index of consistency increases substantially. This can be seen, for example in the motion target case where

$$\begin{aligned} \text{index}(a_0, a_1) &= .312 \\ \text{index}(a_0, a_1, a_3) &= 1.413 \end{aligned}$$

TABLE VI - THE INDEX OF PARAMETER CONSISTENCY

PARAMETERS CONSIDERED	TARGET MOTION	TARGET STATIC	DISTURBANCE MOTION	DISTURBANCE STATIC
$a_0$	.107	.169	.102	.107
$a_1$	.526	.728	.158	.231
$a_2$	.305	.779	.149	.058
$a_3$	2.411	.842	1.415	2.267
$a_0, a_1$	.312	.165	.102	.432
$a_0, a_2$	.224	.175	.103	.100
$a_0, a_3$	1.067	.652	1.075	1.014
$a_1, a_2$	.334	.684	.148	.139
$a_1, a_3$	.632	6.172	.844	.664
$a_2, a_3$	5.304	.961	.960	2.767
$a_0, a_1, a_2$	.283	.177	.732	.475
$a_0, a_1, a_3$	1.413	.372	1.993	1.726
$a_0, a_2, a_3$	.946	3.758	.420	.662
$a_0, a_1, a_2, a_3$	1.565	.586	.668	.147
$a_0, a_1, a_2, a_3$	1.789	.534	.809	.824

this result is to be expected because the integration parameter  $a_3$  (corresponding to an input  $e_0(t)$ ) was by far the most inconsistent parameter. Since this tracking task was compensatory in nature with an input that was randomly appearing to the subjects, one would expect a primary term such as  $a_3$  to be representative of a human's input-output characteristics. Table VI also has some other interesting results. For the motion target case, the combination of parameters which produced the lowest index was a result of only  $a_0$  (or only the input  $e(t)$ ). Referring to the describing function of the human (Figure (9)), this describing function is essentially flat (no lead). From Figure (9) we would conclude that the human is predominately acting as a gain; the model order test in Table VI confirms this fact in the time domain using this modeling approach.

For the static target case, Table VI indicates that the pair  $(a_0, a_1)$  (or the time series  $e(t)$  and  $\dot{e}(t)$ ) are probably the time series that are being processed by the human. With reference to Figure (7) it is observed that a small amount of lead is indicated at the upper frequencies. In this case the frequency results show concurrence with the model order tests.

In the disturbance motion case the results of the index test were not that clear because the values of index  $(a_0)$ , index  $(a_0, a_1)$ , and index  $(a_0, a_2)$  were very close together. From Figure (6) there is a small amount of lead compensation and one would expect this effect to show up in the parameters. This result can be observed by using the parameters in Table III and calculating the ratios  $\frac{a_i}{a_0}$   $i=1,2$ . Using the mean values of the  $a_i$  coefficients,  $i=1,2$  the ratios are illustrated in Table VII.

TABLE VII

	TARGET MOTION	TARGET STATIC	DISTURBANCE MOTION	DISTURBANCE STATIC
$\frac{a_1}{a_0}$	.075600718	.065399526	.257470216	.0798021222
$\frac{a_2}{a_0}$	.0038212637	.008776602	.002750372	.08467249

The ratio  $\frac{a_1}{a_0}$  is the greatest for the motion disturbance case with the ratio  $\frac{a_2}{a_0}$  the smallest. From Table VII the conclusion is that the term  $a_1$  has the most dominant effect in the motion disturbance case. Astron's test which is considered to be more sensitive [13] was used to investigate this aspect further.

In the disturbance static case, the lowest value of the index occurred for the high lead case  $(a_0, a_2)$  which corresponds to using the time series  $e(t)$  and  $\dot{e}(t)$ . Since motion inputs are not available in this task, one would not, in general, expect the human to obtain this type of information from displayed variables. One possible explanation of this effect is the need to reduce the



In the disturbance mode of operation the primary factor was the d.c. gain  $a_0$ . From Table VII, the ratio  $\frac{a_0 DM}{a_0 SM}$  was 2.749. The same ratio the target condition was  $\frac{a_0 NT}{a_0 ST} = .7823$ . These results can be summarized as follows:

DISTURBANCE INPUT

- (1) The d.c. gain  $a_0$  is 2.7 times as high in the motion case as compared to the static case.
- (2) The lead terms  $a_1$  and  $a_2$  are much smaller in the motion case. In the static case, more lead generation is required to compensate for a low d.c. gain. This lead generation must be obtained from the visual display.

TARGET INPUT

- (1) The d.c. gains differed slightly (static is larger than motion).
- (2) There is more lead in the static case than in the motion case. Again, this lead generation must be due to visually displayed signals. To complete this paper, Astrom's test was used to draw some conclusions from a statistical analysis. The test in [1] is based on the ratio  $\Delta$  defined by:

$$\Delta = \frac{J_1 - J_2}{J_2} \cdot \frac{N - n_2}{n_2 - 1}$$

where  $J_1$  and  $J_2$  are values of the loss functional for  $n_1$  and  $n_2$  parameters, respectively and  $N$  is the number of input-output pairs of data points. The variable  $\Delta$  is F distributed with  $n_2 - n_1$ ,  $N - n_2$  degrees of freedom. For  $N = 300$  pairs of data points, if  $\Delta > 3.09$  implies the loss functional has dropped significantly (with 95% probability). If  $\Delta \leq 3.09$ , no conclusions can be drawn. The following tests were conducted to study Figures (10a-d).

score  $\hat{v}$  in equation (11) which has a penalty weighting on  $\ddot{v}(t)$ . From Table VII the ratio  $\frac{a_1}{a_0}$  is greatest for the static disturbance case as compared to the other three conditions. This agrees with the model order test.

Astrom's model order test was applied to Table V and plots of the loss function were obtained. In order to examine Astrom's test, the following values of the cost function were compared.

$$J(a_0) \text{ to } J(a_0, a_1, a_2)$$

$$J(a_0) \text{ to } J(a_1, a_2) \text{ to } J(a_0, a_1, a_2)$$

In this manner we could determine if either  $a_1$  or  $a_2$  was the dominant factor in reducing the output error loss functional. Figures (10a-d) illustrates plots of this test for the four modes of operation.

In figure (10a) for the target motion case the parameter  $a_0$  appears to be the only significant parameter. This concurs with the index of consistency test used previously.

For the target static case the significant parameter appears to be  $a_1$  in lieu of  $a_2$ . This agrees with the index of consistency test and the Bode diagrams. It should be noted that when the human acts as a first order differentiator in the static mode of operation, he is obtaining this information from the visual display of the error signal.

For the disturbance motion case it appears that all three parameters are necessary. The results of Astrom's test are not that definite and it is difficult to draw conclusions. In the disturbance static case the term  $a_2$  has a slightly better effect in reducing the loss functional than  $a_1$ . This is the same result as from the parameter consistency index, however, the conclusion is not that strong. One would expect that in the static disturbance case information of the form  $\dot{v}(t)$  is not available from any motion sensory loop or from the visual display. The slope of Figure (8) is slightly greater than 20 db/decade which indicates differentiation is the greatest for this mode of the experiment.

CASE I - (Target Motion):

Tests

- (1) Compare  $J(a_0)$  to  $J(a_0, a_1)$
- (2)  $J(a_0)$  to  $J(a_0, a_2)$
- (3)  $J(a_0, a_1)$  to  $J(a_0, a_1, a_2)$

CASE II - (Target Static):

Tests

- (1) Compare  $J(a_0)$  to  $J(a_0, a_1)$
- (2)  $J(a_0)$  to  $J(a_0, a_2)$
- (3)  $J(a_0, a_2)$  to  $J(a_0, a_1, a_2)$

CASE III - (Disturbance Motion):

Tests

- (1) Compare  $J(a_0)$  to  $J(a_0, a_1)$
- (2)  $J(a_0)$  to  $J(a_0, a_2)$
- (3)  $J(a_0, a_1)$  to  $J(a_0, a_1, a_2)$

CASE IV - (Disturbance Static):

Tests

- (1) Compare  $J(a_0)$  to  $J(a_0, a_1)$
- (2)  $J(a_0)$  to  $J(a_0, a_2)$
- (3)  $J(a_0, a_1)$  to  $J(a_0, a_1, a_2)$

The results of the test appear in Table VIII.

Astrom's test is very sensitive to  $N$  the number of input-output pairs and a value of  $t < 3.09$  is required to reject the hypothesis that the drop in cost functional is significant (with 95% probability). The larger the value of  $\Delta$ , implies the cost functional has dropped with greater significance (more sensitivity). The results of Astrom's test indicate the following:

DISTURBANCE CONDITION

- (1) For the disturbance static condition, the cost functional does not drop

substantially for any parameter. This result agrees with Figure (10d). Of the four parameters,  $a_2$  appears to have the most sensitive effect on the reduction of the output error loss functional.

- (2) In the disturbance motion case, the variable  $a_2$  had the most sensitive effect (of the four parameters) on the cost functional in tests (2) and (3).

It is noted that in the disturbance conditions the statistical test is somewhat biased because the d.c. gain  $a_0$  changed by almost a factor of 3. Table VII with the normalized ratios provides the best method of comparison of the motion and static disturbance inputs.

TARGET CONDITION

- (1) For the motion target case the terms  $a_1$  and  $a_2$  were not the sensitive parameters. This agrees with the previous tests in which  $a_0$  was determined to be the most significant parameter.

- (2) For the static target case the term  $a_1$  is the most sensitive parameter as indicated by tests (2) and (3). This result is in concurrence with the previous tests and the describing function plots.

The results of these model order tests can be summarized as follows:

- (1) For the motion target case the dominant perceptual variable was  $e(t)$ .
- (2) For the static target case the dominant perceptual variable was  $\dot{e}(t)$ .
- (3) For the static disturbance case, the  $e(t)$  variable was less dominant in the static case but substantially more lead was required. This lead is assumed to come from the visual display.
- (4) In the motion disturbance case, less lead appeared in the human's transfer function. This is an indication that the trackers may be using their motion information to increase their d.c. gain and reduce the requirement of differentiating the displayed error signal.

TABLE VIII - ASTROM'S TEST

TESTS	TARGET MOTION	TARGET STATIC	DISTURBANCE MOTION	DISTURBANCE STATIC
TESTS (1)	17.044	267.020	15.214	5.688
TESTS (2)	27.210	59.759	34.398	10.214
TESTS (3)	17.661	246.066	87.992	7.129

It is noted that the coefficients  $a_0$ ,  $a_1$ , and  $a_2$  obtained in the disturbance condition and the spectra plots obtained here concur with many of the results in the data base obtained by Shirley and Young [14]. This can be seen by the fact that in the disturbance condition, there is a higher d.c. gain in the motion condition as compared to the static condition. In the static disturbance condition, the lower d.c. gain results in more slope in the describing function of the human. These results concur with the earlier spectra results [14] and support the conclusion that roll-motion cues permit the pilot to increase his gain without a loss of system closed-loop stability for the disturbance condition. Using the optimal control model to model the earlier data [14], Curry, et al. [15] treated the vestibular signal strictly as an additional measurement used in the control feedback loop. The same conclusions (i.e. the pilots tendency to increase his gain without a loss of system closed-loop stability) appear as a result of the modeling effort [15].

VIII A Third Method of Validation - Analog Simulation

Since the model developed in this paper shows credibility in both the time domain and in the frequency domain, one would expect that an analog simulation could replace the human in the loop. In an effort to observe how an auto-pilot could replace the man in the loop, a simulation was constructed for the parameters from the target motion condition (table III) and inserted in the loop. Using an analog simulation of the VCS, the autopilot was required to track the IATS for the target input condition. Figure (11a) illustrates the resulting spectrum of

the mean error signal from the data (composed of correlated and uncorrelated parts). Also plotted in figure (11a) is the spectrum of the error signal for the condition of the autopilot in the loop.

From figure (11a) it is easily seen that the correlated spectrum of the error signal from the data and the autopilot appear to match. The uncorrelated portion of the error signal does not match because the autopilot is strictly a deterministic model. Since the input forcing function is deterministic (sum of sines) and the plant was linear, the error signal should have no uncorrelated response. From figure (11a), the -50 db level of  $e_{uncor}$  for the autopilot is due to noise from the analog simulation and the process of computing the spectra.

In an effort to match the two error spectrums, white-gaussian noise passed through a low pass filter was injected at the stick in the autopilot simulation. Figure (11b) show the resulting spectra for the autopilot with the noise inserted in the loop. The power in the noise that was inserted into the loop was determined by the power in the  $e_{uncor}$  spectrum in figure (11a) with the fact that the uncorrelated part of  $e$  can only be due to the white noise as it is passed through the transfer function of the plant. From figure (11b) we see that the autopilot can reproduce similar performance results, if it replaces the man in the loop.

The important point in the autopilot simulation considered here is that in order to describe the human's characteristics, it was necessary to both insert a deterministic model, and in addition, to insert a white noise source to account for the human's randomness.

IX Summary and Conclusions

A study of model order was conducted using statistical analysis and a canonical PID model. The results of the model order test give insight as to which displayed quantity was being used by the human in the tracking task. The data base used in this study was part of a motion study involving humans in a multi axis tracking simulator.

REFERENCES

- [1] Astrom, K. J. and Eykhoff, P., "System Identification-A Survey", Automatica, Vol. 7, pp. 123-162, 1971.
- [2] Junker, A. M., and C. Repligle, "Motion Effects on the Human Operator in a Roll Axis Tracking Task", Aviation, Space and Environmental Medicine, Vol. 46, pp. 819-822, June, 1975.
- [3] Levison, W. H., Baron, S., and Junker, A. M., "Modeling the Effects of Environmental Factors on Human Control and Information Processing", AMRL-TR-76-74, August, 1976.
- [4] Junker, A. M. and Price, D. R., "Comparison Between a Peripheral Display and Motion Information on Human Tracking About the Roll Axis", AIAA Visual and Motion Simulation Conference, Dayton, Ohio, April, 1976.
- [5] Moriarty, T. E., Junker, A. M., and Price, D. R., "Roll Axis Tracking Improvement Resulting from Peripheral Vision Motion Cues", The Twelfth Annual Conference on Manual Control, University of Illinois at Urbana-Champaign, May 25-27, 1976.
- [6] Price, D. R., "A Study of the Effect of Peripheral Vision Motion Cues on Roll Axis Tracking", Master of Science Thesis, Air Force Institute of Technology, December, 1975.
- [7] Repperger, D. W., and Junker, A. M., "PID (Proportional Integral Derivative) Modeling Techniques Applied to Studies of Motion and Peripheral Display Effects on Human Operator Performance", The Twelfth Annual Conference on Manual Control, NASA TRX-73, 170, pp. 703-718, 1976.
- [8] Junker, A. M. and Levison, W. H., "Recent Advances in Modeling the Effects of Roll Motion on the Human Operator", submitted for publication, Aviation, Space, and Environmental Medicine.
- [9] Junker, A. M. and Levison, W. H., "Use of the Optimal Control Model in the Design of Motion Cue Experiments", The Thirteenth Annual Conference on Manual Control, MIT, 1977.
- [10] Levison, W. H., Baron, S., and Krimman, D. L., "A Model for Human Controller Remnant", IEEE Transactions on Man-Machine Systems, Vol. MMS-10, No. 4, December, 1969, pp. 101-106.
- [11] Jex, H. R., Allen, R. W., and Magdaleno, R. E., "Display Format Effects on Precision Tracking Performance, Describing Functions, and Remnant", AMRL-TR-71-63, August, 1971.
- [12] Desai, V. K. and V. W. Fairman, "On Determining the Order of a Linear System", Mathematical Biosciences, Vol. 12, pp. 217-224, 1971.
- [13] Chan, C. W., Harris, C. J., and Wellstead, P. E., "An Order-Testing Criterion for Mixed Autoregressive Moving Average Processes", International Journal of Control, Vol. 20, No. 5, pp. 817-834, 1974.
- [14] Shirley, R. S. and Young, L. R., "Motion Cues in Man-Vehicle Control", IEEE Transactions on Man-Machine Systems, Vol. MMS-9, No. 4, December, 1968, pp. 121-128.
- [15] Curry, R. E., Hoffman, W. C., Young, L. R., "Pilot Modeling For Manned Simulation" AFEDL-TR-76-124, Volume 1, December, 1976.

MAN

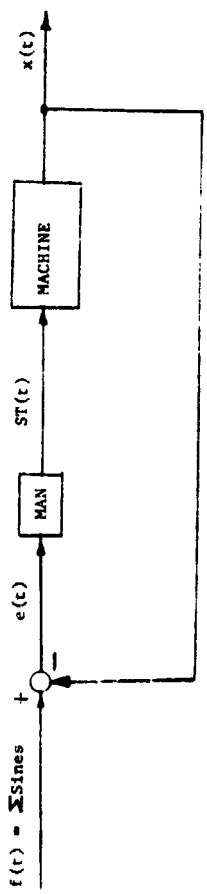


Figure (1a) - The Closed Loop Tracking Task

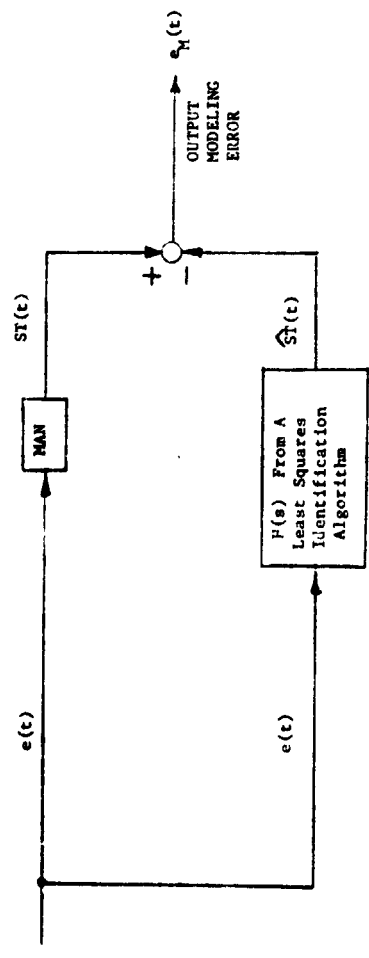


Figure (1b) - The Internal Loop Approach

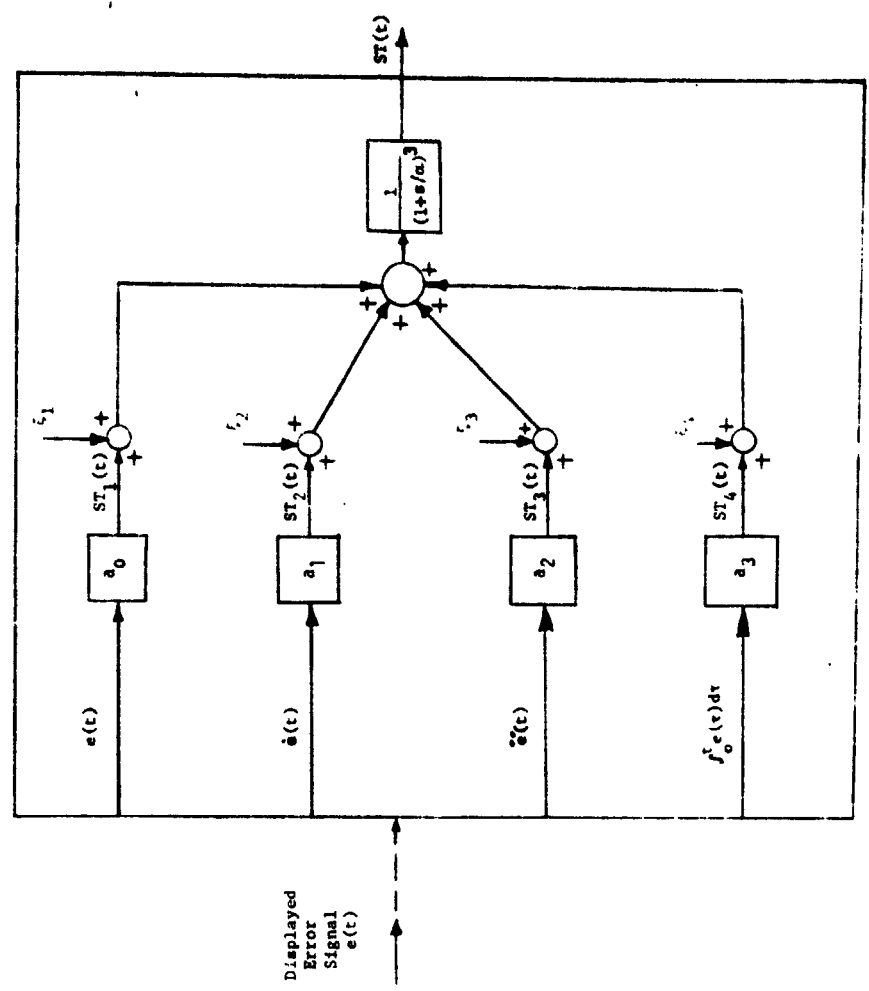


Figure (2) - Man As A Parallel Information Processor

Figure (4) - The Multi Axis Tracking Simulator (MATS)

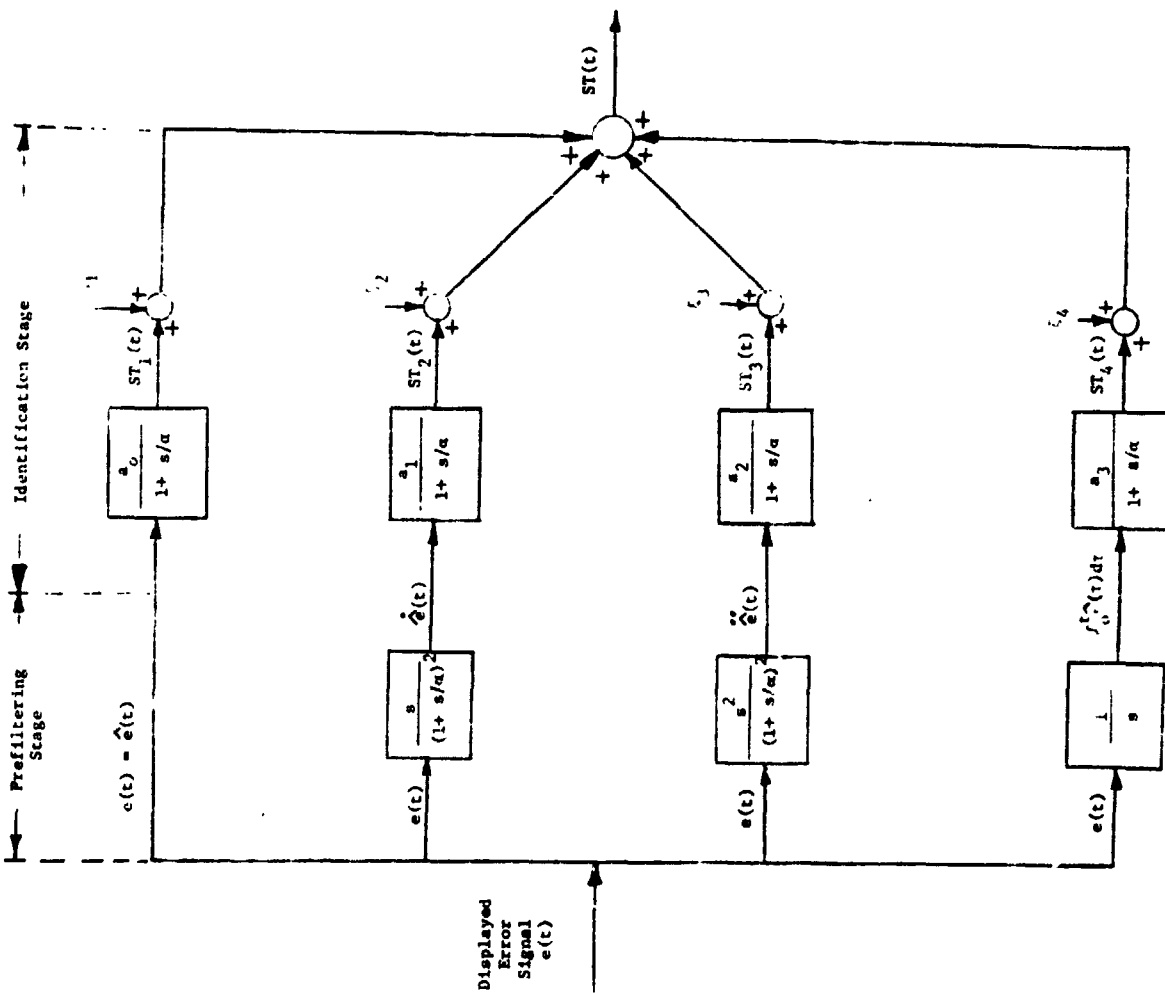
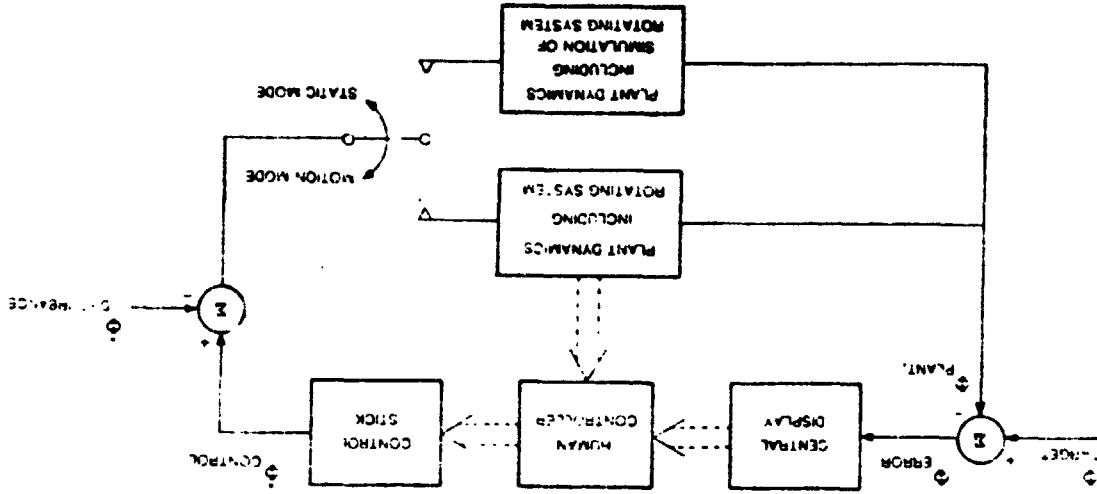
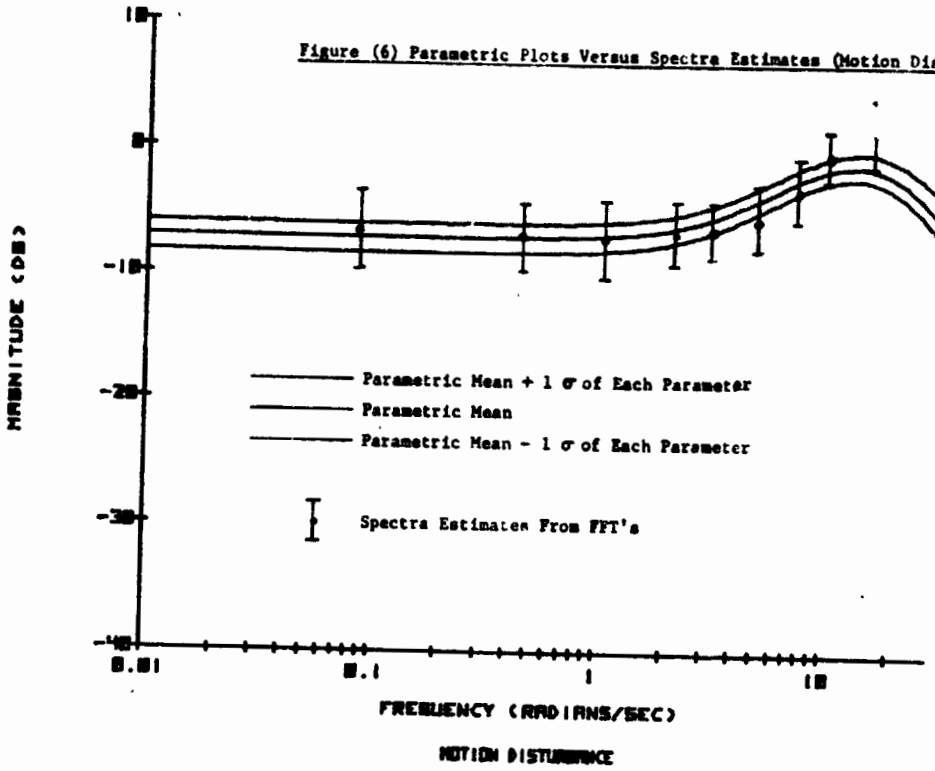


Figure (3)- Implementation of This Identification Approach

Figure (6) Parametric Plots Versus Spectra Estimates (Motion Disturbance Case)



ORIGINAL PAGE IS OF POOR QUALITY

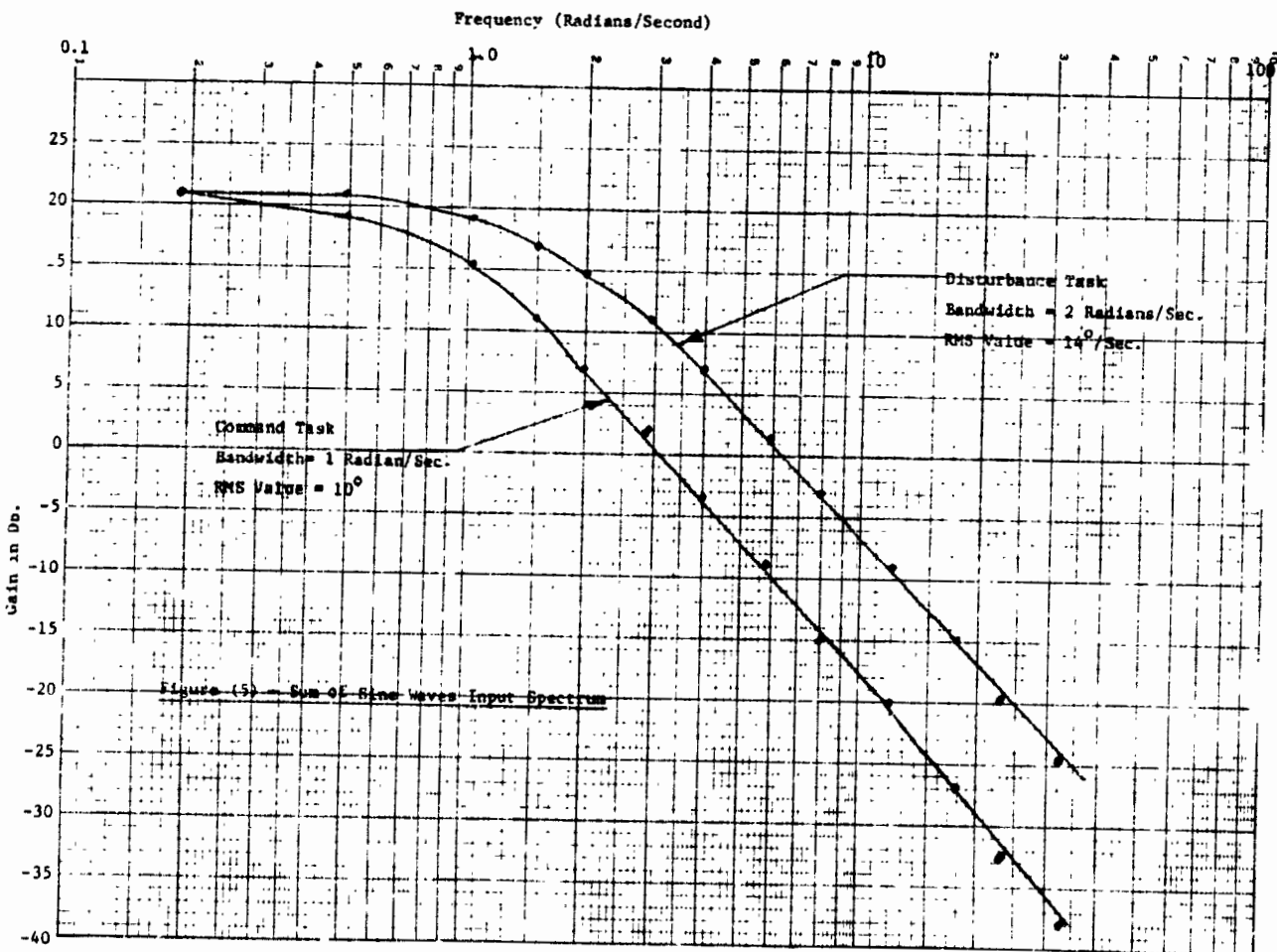


Figure (6) Parametric Plots Versus Spectra Estimates (Static Disturbance Case)

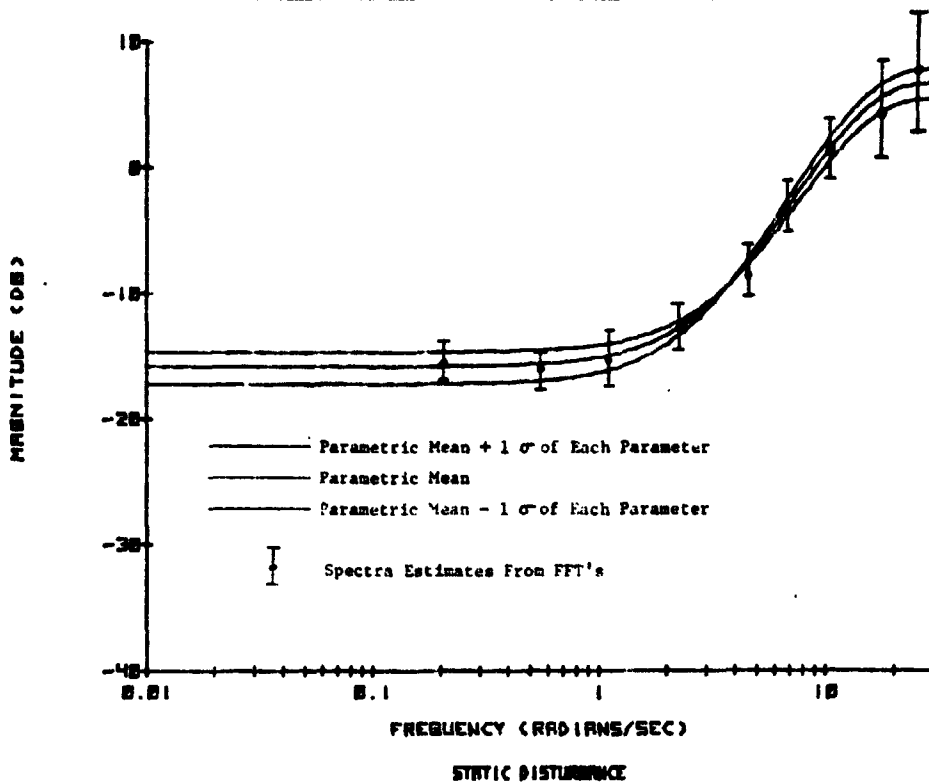
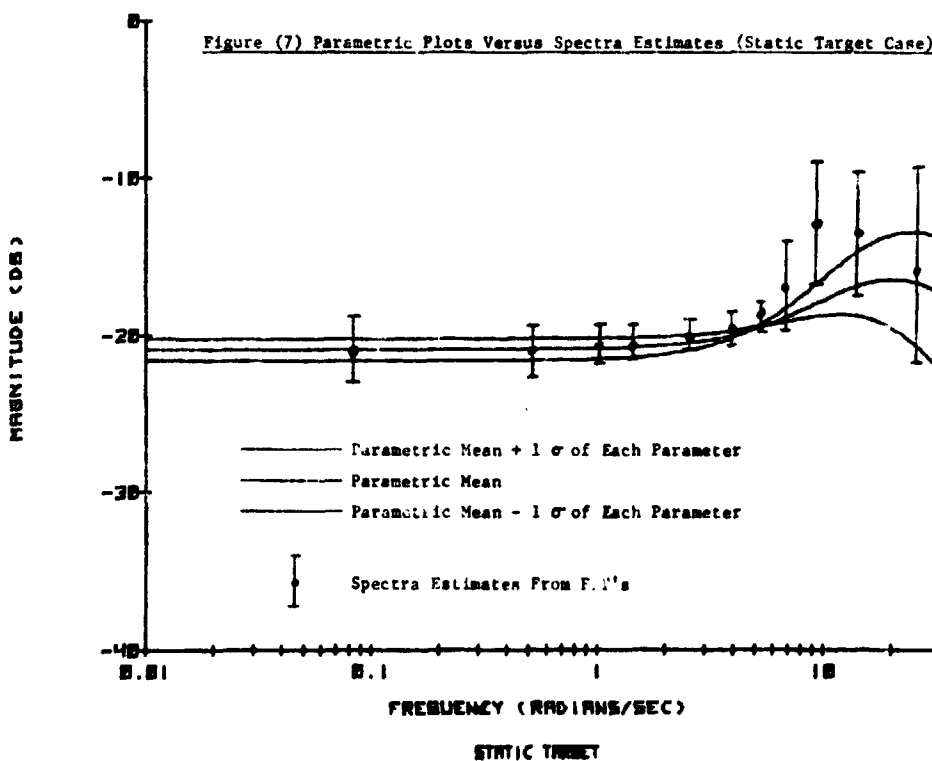
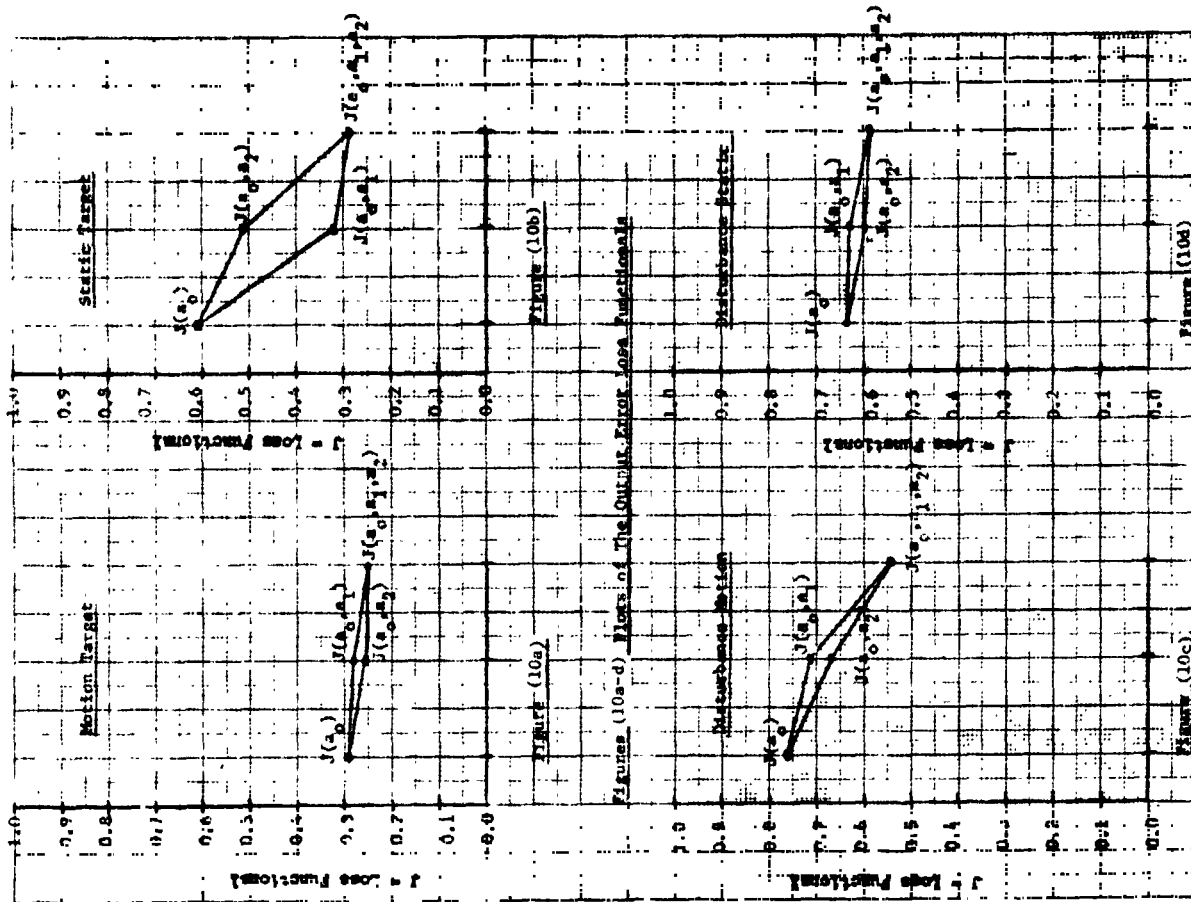


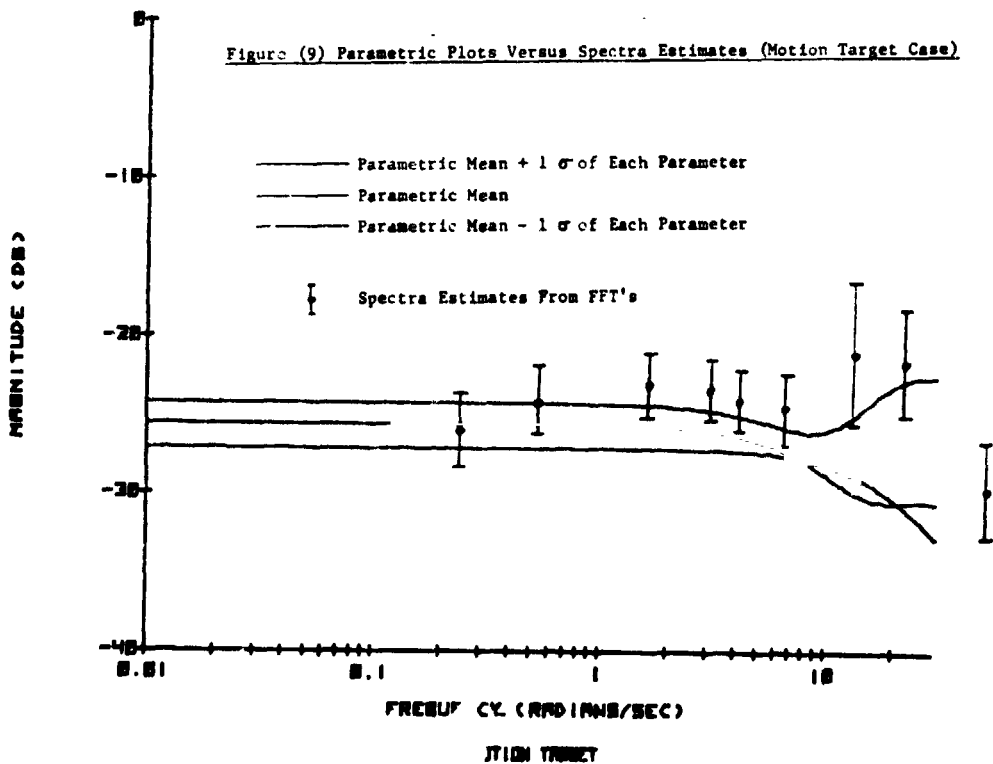
Figure (7) Parametric Plots Versus Spectra Estimates (Static Target Case)

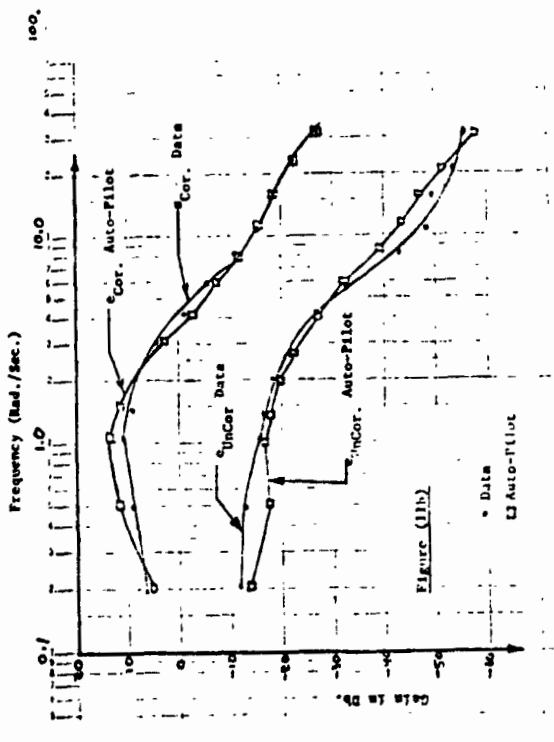
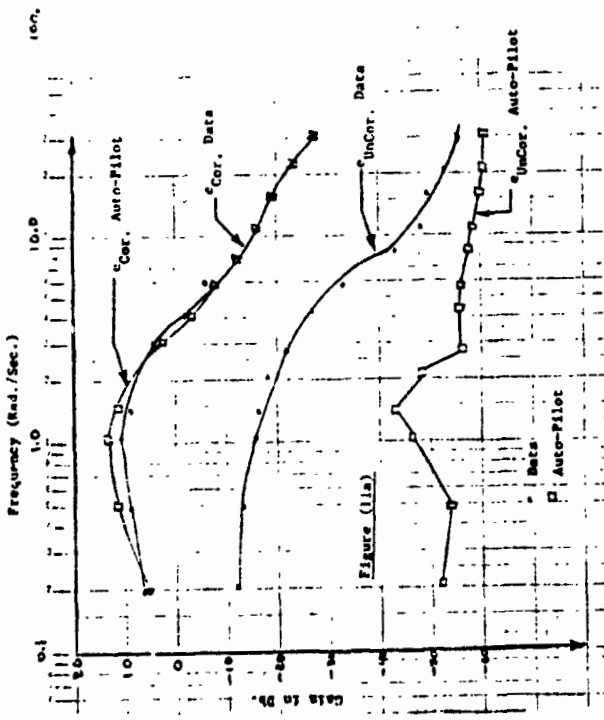






ORIGINAL PAGE IS  
OF POOR QUALITY





ORIGINAL PAGE IS  
OF POOR QUALITY